IMPLEMENTATION OF AN EULERIAN METHOD OF DETERMINATION OF SURFACE WATER COLLECTION EFFICIENCY FOR ATMOSPHERIC ICING PROBLEMS

JANUSZ SZNAJDER

New Technology Center, Aerodynamic Department, Institute of Aviation,
al. Krakowska 110/114, 02-256 Warsaw, Poland, janusz.sznajder@ilot.edu.pl

Abstract

In the presented article numerical implementation of a method of determination of water collection efficiency of a surface in two-phase flow of air and dispersed water droplets of concentration typical for icing problems is presented. An assumption of one-directional coupling between phases, frequently used for similar problems was adopted. In this approach the airflow influences the water droplet phase flow, and itself is not influenced by the droplet flow. Two-dimensional flow model was adopted in Eulerian approach, solving the droplet phase equations of motion in the whole computational domain. The water droplet phase flow was modeled using three variables representing droplet concentration and two components of velocity and three equations: the droplet continuity equation and two equations for the conservation of momentum in two perpendicular directions. The variables and equations describing the motion of the water droplet phase were introduced as User-Defined Scalars and User-Defined Equations to the commercial Fluent solver. It was assumed, that the droplet motion is the result of drag, gravity and buoyancy forces. The test computations were performed for the NACA 23012 airfoil, for two cases of droplet diameter and droplet phase concentration. The computation results were compared with experimental results.

The comparisons demonstrate close agreement of the computed results (mass of captured water in unit time, surface distribution and local maximum value) for low values of Liquid Water Content, defined in FAR25 airworthiness regulations. For higher values of Liquid Water Content, typical for the phenomenon of "Supercooled Large Droplets" the present method overestimates the value of captured water per time, but the maximum value of the collection efficiency and the extent of the surface capturing water is predicted correctly. Also investigations of the effects selected aerodynamic and flow parameters on the mass of collected water were conducted.

Keywords: two-phase flows, computational fluid dynamics, water collection.

Water collection efficiency of an aerodynamic surface is a measure of the amount of water hitting the surface in two-phase flow consisting of air and water droplets. It is defined as ratio of water stream intercepted by an infinitesimally small surface element to the value of water stream far away from the surface. Evaluation of this quantity is one of the tasks involved in the simulation of the process of ice accretion on surfaces exposed to icing conditions, particularly on surfaces generating aerodynamic forces (wings, control surfaces) and engine inlets. Because of the importance of this quantity for the simulation of the icing process and its influence on aerodynamic characteristics of aircraft this subject deserves attention, and this concerns the computational methods applicable for the aerodynamic surfaces exposed to icing condition and their results in icing condition defined by airworthiness regulations. The present work is an element of the implementation of the methodology of the simulation of ice accretion on aerodynamic surfaces and its prevention which involves also other tasks, such as simulation of the water film flow and heat transfer on its surface, determination of the freezing fraction and regeneration of the computational grid on surface deformed by ice. The present work concentrates, however, on the interception of water by an aerodynamic surface in two-phase flow.

Two approaches have been used in numerical computations of water collection efficiency of an aerodynamic surface. Chronologically the first of them is an Lagrangian approach, tracking the motion of a droplet in space. It requires the determination of a "source zone" of water droplets hitting the surface. By the calculation of the trajectories of individual droplets leaving the source zone it is possible to determine the local collection efficiency as the ratio of the distance between the source points of two closest droplets in the source zone (farfield) and the distance of their impact points along the airfoil surface. This approach has been popular in the first ice accretion simulation codes using potential model of air flow. Its constraints appear in the application for multi-element airfoils and three-dimensional surfaces, where the source zones for droplets reaching wing surface have more complicated shape than in the two-dimensional, single-element airfoil case. In recent years, particularly in the last decade, the task of determination of water collection efficiency is being done more often using an Eulerian approach. In this approach the water dispersed in droplets is regarded as continuous phase and the solution of droplet motion is being obtained simultaneously for all the points of the computational domain. In this approach there is no need for the determination of the source zone for droplets hitting the surface. Instead the droplet flow field is determined simultaneously in the whole computational domain by the solution of the continuity and momentum equations for the water phase with aproppriate boundary and initial conditions. This approach is analogous to the determination of air flow field using Euler or RANS equations of fluid dynamics and became competitive to the Lagrangian approach as the solutions of Euler and RANS equations became affordable means of solution of practical design problems in the industry. In many cases the solution of air and water flow is being conducted using different computational codes. This is possible because of the frequently adopted assumption that the droplet flow does not affect the air flow. With this assumption it is possible to conduct a solution of water flow for a steady case using a converged, steady solution of air flow. In the present case similar assumption regarding the one-directional influence of air flow on droplet flow has been applied. With this assumption a model of two-phase flow with boundary conditions for external flow has been built and implemented as extension of the ANSYS FLUENT solver using provided with the solver means of introducing user-defined variables and transport equations.

FLOW EQUATIONS

The air flow equations consists of equations of continuity, components of momentum, energy and turbulence (one equation Spalart-Almaras turbulence model) and are being solved by Fluent [1] solver in identical way as in one-phase fluid case. For the present work the pressure-based solver was selected with second order upwind discretisation of flow variables and SIMPLE-type pressure-velocity coupling.

The water droplet flow equations consist of the continuity equation:

$$\frac{\partial \rho_d}{\partial t} + \vec{\nabla} \cdot \rho_d \vec{U}_d = 0 \qquad (1)$$

and the momentum equation, written in vector form:

$$\frac{\partial \rho_d \vec{U}_d}{\partial t} + \vec{\nabla} \cdot (\rho_d \vec{U}_d) \vec{U}_d = \vec{f}_d + \rho_d (1 - \frac{\rho_a}{\rho_w}) \vec{g} - \frac{\rho_d}{\rho_w} \cdot \vec{\nabla} p \qquad (2)$$

where:
$\vec{U}_d$ – droplet velocity,
ρ_d – droplet concentration, equal to $\alpha \cdot \rho_w$,
α – water volume fraction,
ρ_w – water density,
ρ_a – air density,
$\vec{f}_d$ – drag force,
$\vec{g}$ – gravitational acceleration.

The first terms in equations (1) and (2) describe unsteady flow and are omitted in the implementation of the steady flow case. The divergence terms are treated as follows:

The Fluent solver provides the possibility of computing the transport of a user-defined scalar ϕ_k solving the equation (for the steady case):

$$\nabla \cdot (\vec{\psi} \phi_k - \Gamma_k \cdot \phi_k) = S_{\phi k} \qquad (3)$$

where $\vec{\psi}$ is a vector field and Γ_k diffusion coefficient of the scalar "k". In the default case $\vec{\psi} = \rho \vec{U}$, where $\vec{U}$ is fluid velocity, computed for the single-phase flow.

In the present, two-dimensional case, three scalars have been used to represent three variables: ρ_d, u_d, and v_d, where u_d and v_d are components of the droplet velocity $\vec{U}_d$. For each of them Equation (2) is solved in the computational domain. The components of the $\vec{\psi}$ vector are the products $\rho_d u_d$ and $\rho_d v_d$. The scalar Γ in Equation (2) is set to zero, in order to comply

with Equations (1) and (2). The computation of the advection terms in equation (1) and (2) is being accomplished in an user-defined procedure, integrating the advection term in Equation (3) over the cell volume. This is done applying Gauss' divergence theorem (integration over cell faces of the dot product of the $\vec{\psi}$ vector and wall normal vector). The wall values of the $\vec{\psi}$ vector components are computed using an upwind scheme, based on cell center values and gradients of scalars computed at the cell centers. For the boundary cells the wall values of the scalars are set as boundary conditions.

The forces acting on the droplets taken into account include droplet drag, net effect of gravity and buoyancy and effect of pressure gradient in the flow field. This is what most researches take into account, e.g. [2, 3]. Drag force is computed using formula proposed by Morrison [4] for a sphere, because of reported agreement with experimental data for a wide range of droplet Reynolds number (Figure 1).

$$C_D = \frac{24}{Re} + \frac{2.6\left(\frac{Re}{5.0}\right)}{1+\left(\frac{Re}{5.0}\right)^{1.52}} + \frac{0.411\left(\frac{Re}{263,000}\right)^{-7.94}}{1+\left(\frac{Re}{263,000}\right)^{-8.00}} + \left(\frac{Re^{0.80}}{461,000}\right)$$
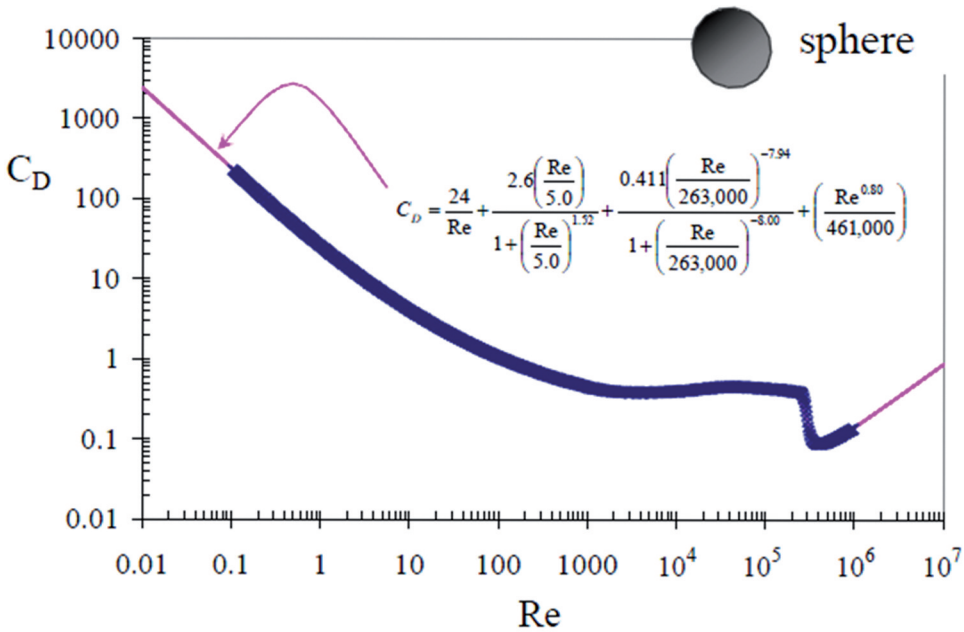
Fig. 1. Comparison of analytical formula for droplet c_D with experimental data [4]

Choosing an appropriate formula for droplet c_D is, however, not a trivial task, since the results of formulas used by different researchers for the droplet Reynolds number range occuring in the computations of droplet flow ($0 \leq Re \leq {\sim}1000$) differ significantly (Figure 2). Perhaps more experimental research is still needed in this field.
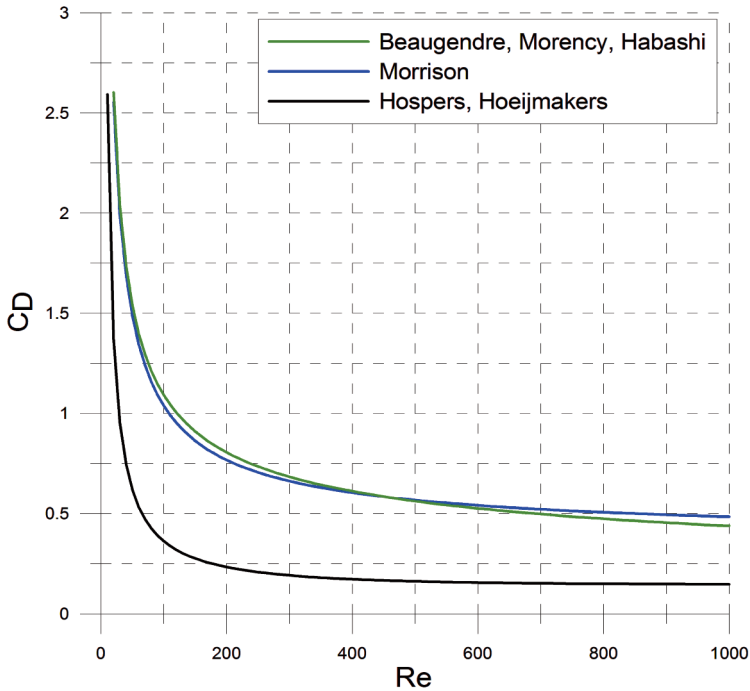
Fig. 2. Comparison of droplet c_D computed with formulas used by Beaugendre et al. [2], Morrison [4] and Hospers, Hoeijmakers [3]

BOUNDARY CONDITIONS

Boundary conditions for the droplet flow have been chosen to correspond to the external flow boundary conditions being used for the computation of the aerodynamic characteristics of airfoils and three-dimensional bodies. The external border surfaces of the computational domain have been divided into two categories: pressure farfield and pressure outlet. The pressure farfield includes surfaces of uniform and undisturbed flow lying ahead of and on both sides of the airfoil. The air flow quantities being set there include Mach number, X and Y components of the vector of the flow direction, pressure and temperature. They allow for the determination of the values of the flow variables computed by the solver: components of flow velocity, density, pressure and temperature. The water flow variables include mass concentration and X and Y components of the droplet velocity. It is assumed that the X and Y components of the air and water droplet velocity are equal in the far field (The computational problem may be considered as body moving through two-phase fluid at rest). On the outlet surface only the pressure and temerature are set. The air flow velocities and density include disturbances caused by the airfoil and are computed by the solver. Similarly the water flow concentration and velocity components are computed by the solver up to the cell center point adjacent to the outlet surface. Their values on the outlet surface are extrapolated using gradients computed in the center of the cell.

On the airfoil surface the typical wall no-slip boundary condition is applied for the air flow. For the water flow there are two cases treated in different way: the case when water is intercepted by the surface and the case when water droplets move by the surface. In the first

case, when $(\vec{U}_d \cdot \vec{n}) < 0$, $\vec{n}$ being the cell-wall normal vector, the airfoil surface is considered totally permeable for the water. The water velocity on the surface is extrapolated using gradients computed in the cell center. This is a standard procedure applied for the computation of collection efficiency for the simulation of ice accretion. The flow of water on the surface is a separate problem, being treated in the ice accretion simulation codes with the application of heat exchange and heat balancing procedure, summing heat flows in and out of the surface. This allows for the determination of the amount of water that freezes in particular location or runs away along the surface. Such procedure has not been created for the present work yet, but is planned for the future.

In the case when $(\vec{U}_d \cdot \vec{n}) > 0$ the water concentration on the surface, ρ_d is set to zero, and the components of water flow velocity are extrapolated using gradients computed at the cell center. This ensures the continuity of droplet flow variables. The boundary conditions have been summarized in Table 1.

Table 1. Summary of boundary conditions for dispersed water phase [3]

ZONE	BOUNDARY CONDITIONS
Farfield	$\vec{U}_d = \vec{U}_a$, $\rho_d = \rho_{d\inf}$
Outlet	$\vec{U}_d, \rho_d$ extrapolated on cell border face using gradients computed at the cell center
Airfoil, case $(\vec{U}_d \cdot \vec{n}) < 0$	$\vec{U}_d, \rho_d$ extrapolated on cell border face using gradients computed at the cell center
Airfoil, case $(\vec{U}_d \cdot \vec{n}) > 0$	$\vec{U}_d$ extrapolated on cell border face using gradients computed at the cell center, $\rho_d = 0$

RESULTS OF COMPUTATIONS

In order to compare the present method with experimental results, two computational cases were created for comparison with experimental data using NACA 23012 airfoil of chord equal 0.9144 m, at the angle of attack α = 2.5°. Free stream velocity was 78.23 m/s, far field pressure and temperature was 101330 Pa and 299 K respectively. In the first case Liquid Water Content (LWC, equal to ρ_d far away from the airfoil) was set at 0.19 g/m³ and was 20 μm. In the second case LWC was 1.89 g/m³ and droplet diameter 236 μm. The conditions have been chosen for the experiment in [5]. The results of experiment, quoted in [3] represent measured distribution of collection efficiency of a set of droplet sizes with Median Volumetric Diameter of 20 μm and 236 μm. The computed distribution of dispersed phase density, ρ_d around the airfoil is presented in Figure 3 and the computed characteristics of airfoil collection efficiency is shown in Figure 3.

The results show that only the airfoil nose region is being hit by the droplets. The predicted maximum value of β is approximately 10% higher than the value obtained in experiment. The integrated value of collection efficiency β over the impingement area obtained with

the present method is 0.0230 m^2 whereas for the experimental data it equals 0.02385 m^2. The agreement is quite good, as the difference between the results is about 3.5% of the experimental value.

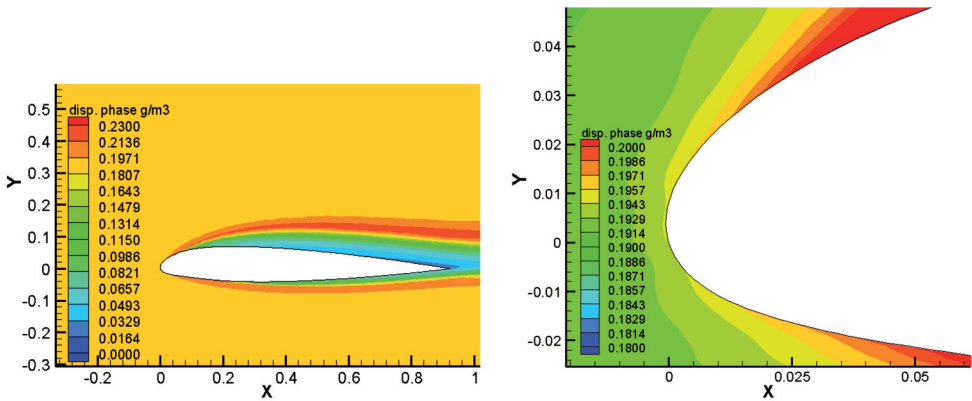Fig. 3. Contours of droplet phase density, ρ_d around NACA 23012 airfoil, at angle of attack α = 2.5°
[J. Sznajder − opracowanie własne]

There are other differences between the experimental and computational results in Figure 4: a steeper shape of the computational distribution of collection efficiency than the experimental one, and a shift of the point of maximum β in the direction of positive values of "s" coordinate, compared to the measured position of the maximum β.
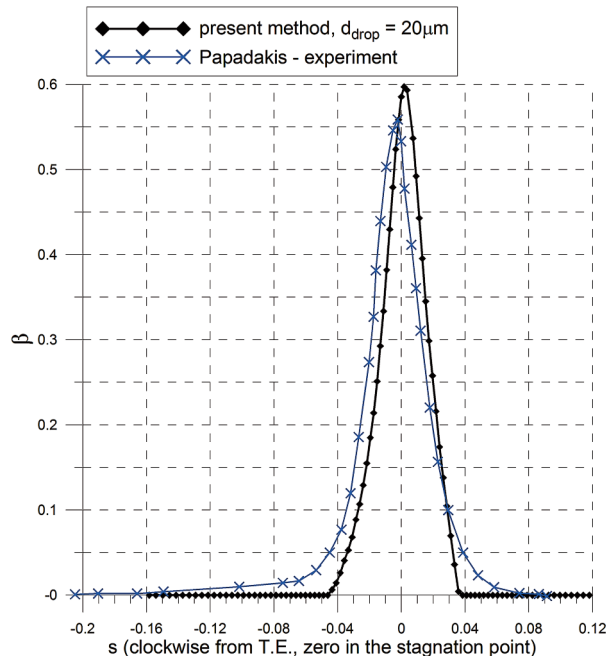
Fig. 4. Comparison of the distribution of collection efficiency computed with the present method and results of an experiment for the case with droplet diameter of 20 μm around the airfoil circumference-s. The S-coordinate has negative values on lower side of airfoil, from the trailing edge to stagnation point and positive values for upper side of the airfoil [J. Sznajder − opracowanie własne]

The first effect is likely due to the presence of droplets of different diameters in the experiment, while the computations were performed for one droplet diameter, 20 μm. Results of computations for "bins" of droplets of different diameters in [3] show flatter shape of the β-characteristics for low values of β. The explanation for this is such, that larger, heavier droplets are not deflected by the flow as much as small droplets and hit the surface in regions where the small droplets are moved away with the flow.

The second effect, the shift of the point of maximum β might be due to error in the measurment of its position in the experiment. Its location in the stagnation point is rather unlikely, since the position of the stagnation point is the result of the circulation of the air around the airfoil. The droplets are set in motion by the drag force which is the result of the movement of air relative to droplets and its magnitude is dependent of the difference of air and droplet velocity. When reaching the airfoil surface, droplets have different velocity, in magnitude as well as in direction. Considering this, one should expect the position of maximum β at a point where droplets hit the surface at the right angle, which is located somwhere between the tangent to the airfoil, with normal vector inclined to chord at the airfoil angle of attack (point A, Figure 5), and the stagnation point (point S). In the present computations the position of the point of maximum β was predicted at the point B (Figure 5). The values of static pressure and collection efficiency at points A, B and S are shown in Table 2.
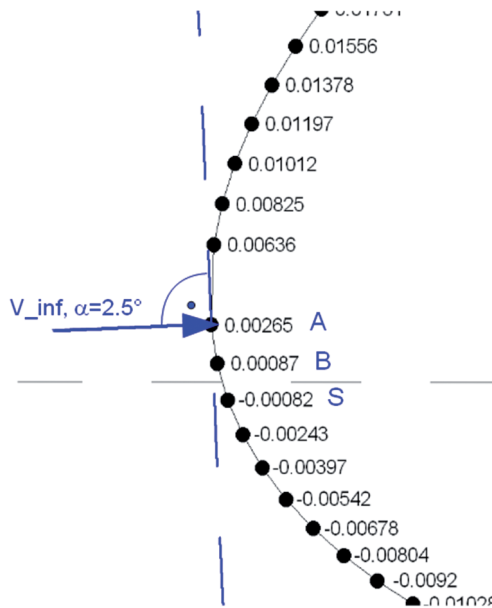

Fig. 5. Region of maximum value of the collection efficiency on airfoil.
Point labels are point Y-coordinates [J. Sznajder – opracowanie własne]

Table 2. Pressure and collection efficiency values for points around the point of maximum β [J. Sznajder – opracowanie własne]

Point designation	X-coordinate [m]	Y-coordinate [m]	S-coordinate [m]	Pressure [Pa]	β
A	-0.00050	0.00265	0.00357	104745.00	0.59402
B	-0.00020	0.00087	0.00176	104965.20	0.59786
S	0.00030	-0.00082	0.0	104989.20	0.58604

The collection efficiency for the second case, for droplet diameter of 236 µm is presented in Figure 6. In this case the main difference between the results of computations and experiment is the overestimation of the collection efficiency, but the character of changes of β is in good agreement on both sides of the stagnation point. Similar overestimation of computational results over the same experimental results was reported in [3] where computations of the air flow were performed with a potential-flow model and the droplet flow was computed using Eulerian approach. This difference is explained in [3] by the splashing of large droplets on contact with the airfoil surface which leads to rebound of smaller droplets off the surface back into the flow. The value of collection efficiency integrated over the impingement area obtained with the numerical method is 0.1045 m^2 and is more than twice the value calculated for the experimental data, which is 0.0482 m^2. In this case of large droplets there is need for more precise modelling of the behavior of droplets in contact with the surface and the splashing of droplets. It is also worth noting, that the value of droplet diameter of 236 µm is an example of very rarely ocurring phenomenon of Supercooled Large Droplets, well in excess of intermittent icing conditions defined in airworthiness regulations FAR 25 (Figure 6).
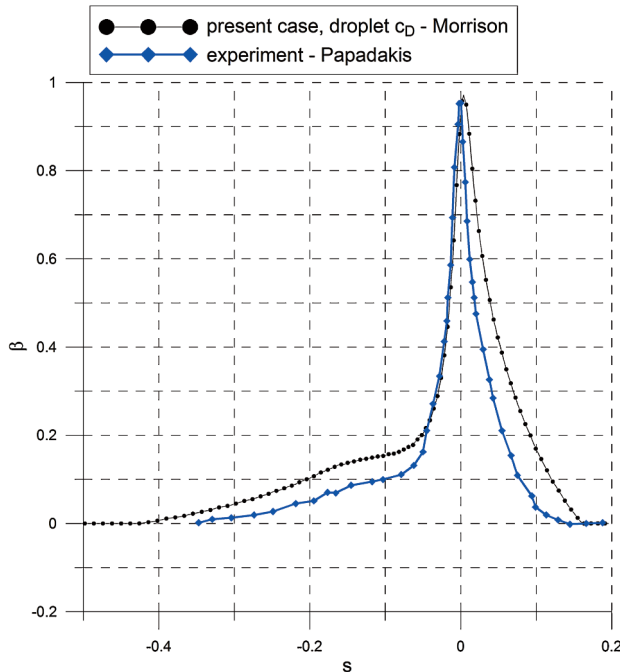

Fig. 6. Comparison of the distribution of collection efficiency computed with the present method and results of an experiment for the case with droplet diameter of 236 µm around the airfoil circumference-s [J. Sznajder – opracowanie własne]

The airworthiness regulations, FAR25, appendix C [6] define icing conditions in terms of droplet median diameter against liquid water content for different temperature values (Figure 7). It is therefore interesting to compare the results of mass flux of collected water computed for a single-diameter approximation of droplet distribution with results for different distributions of droplet size, since the computations for a single-droplet approximation of the droplet phase flow require much less time and resources than computations for a distribution of droplet size. For this purpose the mass flux of collected water computed for single droplet distributions

and conditions defined by t = -20°C and diameter of 20 µm in stratiform clouds (Figure 7), was compared with results obtained for three normal distributions of droplet size, each with medium diameter of 20 µm, diameter range of <0 - 40 µm> and different values of standard deviation σ (Figure 9).

Mass flux of collected water for a given value of σ was obtained as weighted sum of fluxes computed for each diameter indicated with a dot in graphs of Figure 8, obtained through the integration of the β characteristics over the airfoil surface. The values of the fraction of total LWC corresponding to given β characteristics were used as weighing coefficients. The results of computations are presented in Figure 9. They indicate, that for the determination of mass of water collected by an airfoil, in conditions defined by the FAR 25 regulations (Figure 7) a single-diameter droplet distribution model is justified.
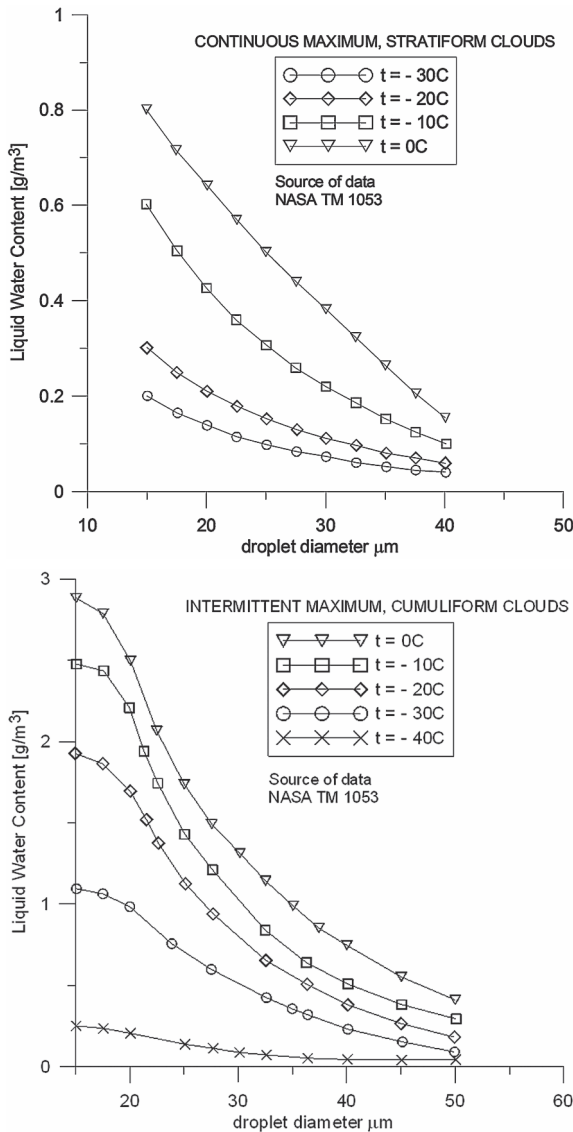

Fig. 7. Definition of continuous and intermittent icing conditions, FAR25 regulations, appendix C [6]
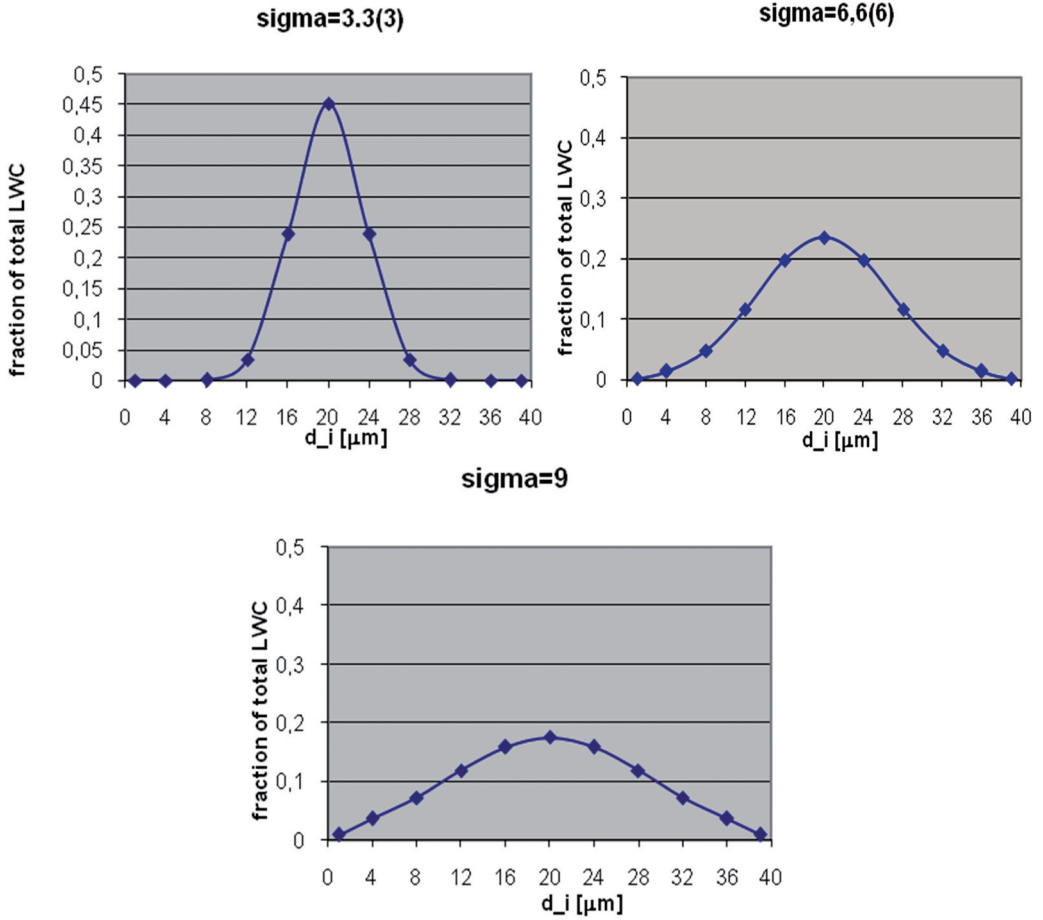
sigma=3.3(3)

sigma=6,6(6)

sigma=9

Fig. 8. Distributions of droplet diameter [J. Sznajder − opracowanie własne]

results for normal distribution of d_{drop}, different standard deviation values
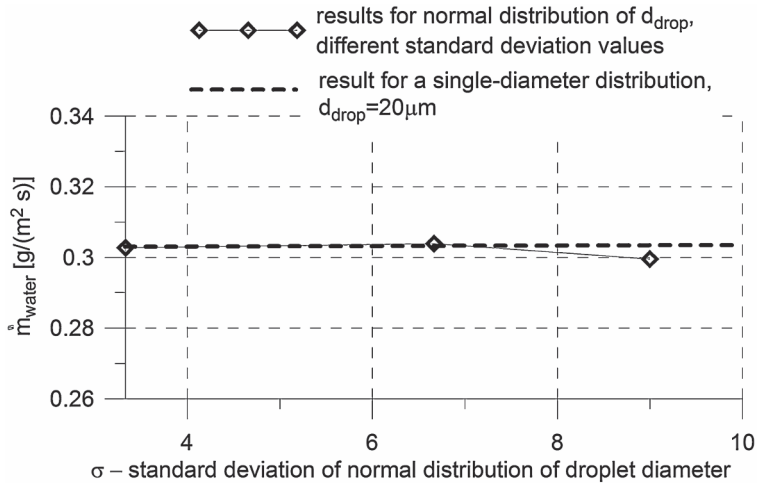
result for a single-diameter distribution, $d_{drop}=20\mu m$

Fig. 9. Mass flux of water collected by airfoil at different values of σ. NACA 23012 airfoil at $\alpha = 2.5°$, M = 0.22, Re = 4.5 mln, LWC = 0.2 g/m^3 [J. Sznajder − opracowanie własne]

For the icing conditions defined for stratiform clouds in Figure 7 computations were performed to determine the values of diameters of droplet transporting most of the water to an airfoil. The results, presented in Figure 10 show, that at temperatures between 0°C and -10°C most of the water hitting the airfoil is transported by droplets of diameters between 20 and 30 μm. At low temperatures, close to -20°C the mass of collected water is more independent of droplet diameter.
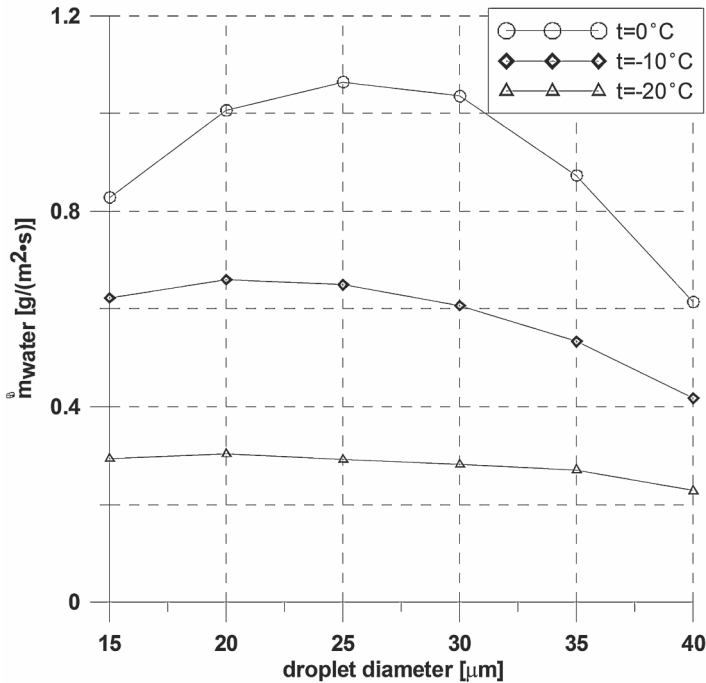

Fig. 10. Dependence of mass of collected water on droplet diameter for icing conditions definedby FAR 25 regulations, Appendix C. NACA 23012 airfoil at α = 2.5°, M = 0.22, Re = 4.5 mln [J. Sznajder – opracowanie własne]

Investigations of the effect of flight parameters: angle of attack and Mach number on the mass of collected water were also conducted. Computations for different values of angle of attack were done for NACA 23012 airfoil at Mach number of 0.22 and Reynolds number of 4.5 mln using single-diameter approximation for the droplet phase. Figure 11 shows distributions of the collection efficiency β computed for the range of angle of attack values from 2.5° to 11°. A tendency of decreasing the peak value and increasing the area hit by the droplets as the angle of attack is increased is visible. Also the point of peak value of β moves slightly towards the bottom side of the airfoil, following the stagnation point. In Figure 12 dependence of the mass flux of collected water on the angle of attack is shown. The results were obtained for two conditions of temperature and Liquid Water Content, according to FAR 25, appendix C: 0°C, 0.19 g/m^3 and -20°C, 0.635 g/m^3. In both cases the angle of attack of minimum captured water coincides approximately with minimum of profile drag. There is no rapid growth of the mass of the captured water when angle of attack is increased within the investigated α-range. Mass flux of captured water at α = 11° is approximately 30% higher than its minimum at α = 1~2. Figure 10 shows the effect of Mach number change on the mass of captured water and maximum value of β ocurring at Mach number of 0.5. The mass of captured water per second increases with growing Mach number which is due to growing air velocity.
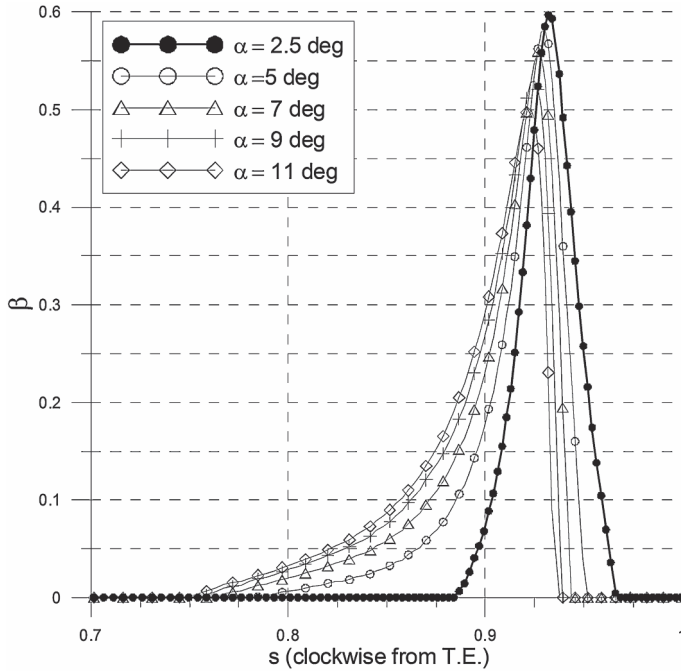
Fig. 11. Water collection efficiency characteristics obtained for different angles of attack for NACA 23012 airfoil at $\alpha = 2.5°$, M = 0.22, Re = 4.5 mln, LWC = 0.2 g/m^3, t = -20°C, d_{drop} = 20 µm [J. Sznajder – opracowanie własne]
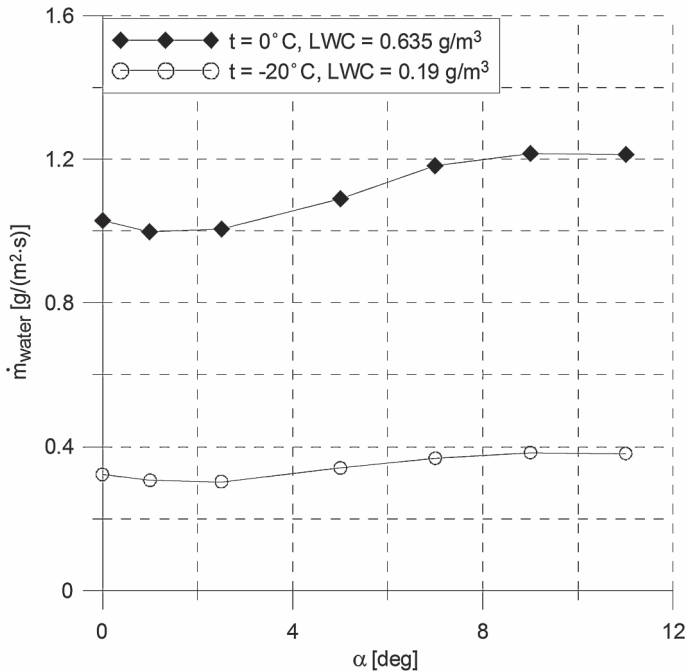

Fig. 12. Dependence of mass flux of collected water on the angle of attack for two sets of icing conditions. Results obtained for NACA 23012 airfoil at $\alpha = 2.5°$, M = 0.22, Re = 4.5 mln, LWC = 0.2 g/m^3, t = -20°C and t = 0°C [J. Sznajder – opracowanie własne]
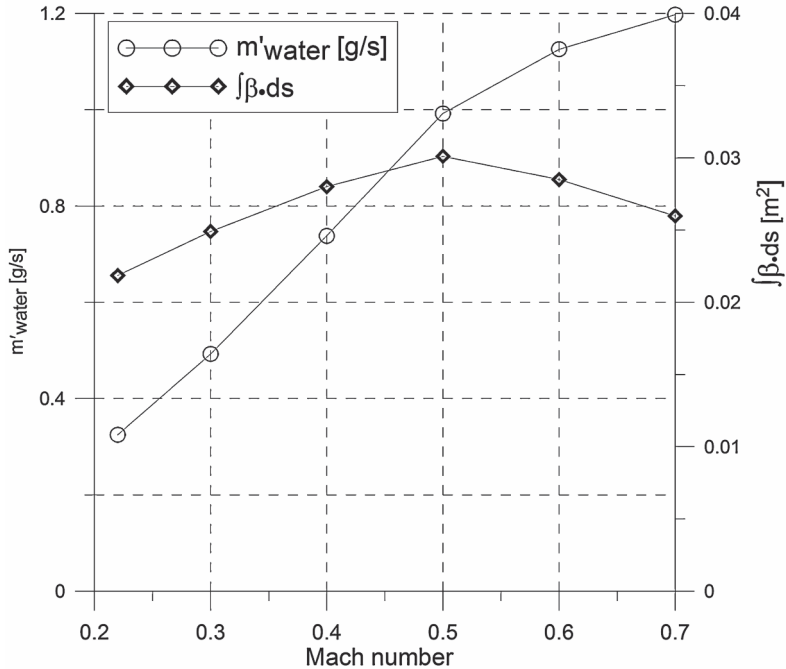
Fig. 13. Dependence of the maximum value of collection efficiency β and mass flux of captured water on Mach number. Results obtained for NACA 23012 airfoil at α = 2.5°, LWC = 0.2 g/m³, t = 0°C

[J. Sznajder – opracowanie własne]

CONCLUSIONS

The proposed method of evaluation of collection efficiency of an aerodynamic surface, based on one-way coupling between air flow and dispersed water phase flow produces results in reasonable agreement with experimental data for droplet dimensions and Liquid Water Content of clouds within values defined in FAR 25 regulations, appendix C. For higher values of droplet diameter and LWC, typical for Supercooled Large Droplets the collection efficiency is overestimated. Nevertheless, the method is flexible enough to evaluate the impact of the most important aerodynamic and atmospheric parameters on the collection efficiency, such as: angle of attack, flight speed, cloud Liquid Water Content and droplet diameter. The addition of model for droplet splashing in contact with surface should improve its accuracy for large droplets. Future work will address the simulation of water film flow and ice accretion on the wing surface.

REFERENCES

[1]   Fluent Inc. (2006). FLUENT 6.3 User's Guide.
[2]   Beaugendre, H., Morency, F., Habashi, W.G. (2003). FESNSAP-ICE's Three-Dimensional In-Flight Ice Accretion Module: ICE3D, *Journal of Aircraft*, Vol. 40, No. 2.
[3]   Hospers, J. M., Hoeijmakers, H. W. M. (2010). Numerical Simulation of SLD Ice Accretions, 27th International Congress of the Aeronautical Sciences.
[4]   Morrison, F. A. (2011). *Data Correlation for Drag Coefficient for Sphere*, Department of Chemical Engineering, Michigan Technological University, Houghton, MI, www.chem.mtu.edu/~fmorriso/DataCorrelationForSphereDrag2010.pdf, October 2011.

[5] Papadakis, M., Rachman, A., Wong, S.-C., Yeong, H.-W., Hung, K. E, Vu, G. T., Bidwell, C. S. (2007). Water droplet impingement on simulated glaze, mixed and rime ice accretions. Technical Report NASA/TM-2007-213961, NASA, October 2007.

[6] *Federal Aviation Regulations FAR 25 Appendix C*, http://www.flightsimaviation.com/data/FARS/part_25-appC.html.

IMPLEMENTACJA EULEROWSKIEJ METODY WYZNACZANIA OSADZANIA SIĘ WODY NA POWIERZCHNI W ZAGADNIENIACH DOTYCZĄCYCH OBLODZENIA

Streszczenie

W pracy przedstawiono implementację numeryczną metody wyznaczania współczynnika masy wody uderzającej w powierzchnię w dwufazowym opływie powietrza i rozproszonych kropel wody o koncentracji typowej dla sytuacji spotykanych w problemach związanych z oblodzeniem atmosferycznym. Przyjęto często stosowane założenie o jednokierunkowym sprzężeniu przepływów, tzn. że przepływ powietrza oddziałuje na przepływ fazy wodnej natomiast przepływ fazy wodnej nie ma wpływu na przepływ powietrza. Przyjęto dwuwymiarowy model zjawiska w ujęciu Eulerowskim, rozwiązując równania przepływu fazy wodnej w całym obszarze obliczeniowym. Przepływ fazy wodnej zamodelowano przez wprowadzenie trzech zmiennych reprezentujących koncentrację fazy i dwie składowe prędkości przepływu oraz trzech równań: równania ciągłości fazy wodnej i dwóch równań zachowania składowych pędu w kierunku dwóch osi układu współrzędnych. Zmienne i równania opisujące ruch fazy wodnej wprowadzono jako Skalary Definiowane Przez Użytkownika i Funkcje Definiowane Przez Użytkownika w komercyjnym programie obliczeniowym Fluent. Założono, że ruch fazy wodnej jest wynikiem działania sił: oporu, ciężkości i wyporu na krople wody. Przeprowadzono obliczenia testowe dla opływu profilu NACA 23012 i dwóch przypadków wartości średnicy kropel i koncentracji fazy wodnej. Uzyskane wyniki porównano z wynikami eksperymentu. Wyniki porównań wykazują dobrą zgodność uzyskanych wyników (masy osiadającej wody na jednostkę czasu, rozkładu powierzchniowego i maksymalnej wartości) dla umiarkowanych wartości zawartości rozproszonej wody w powietrzu, opisanych przez regulacje FAR 25. Dla zawartości wody znacznie przekraczającej te wartości, typowych dla zjawiska „Supercooled Large Droplets" prezentowana metoda przeszacowuje wartość przechwytywanej wody, ale prawidłowo wyznacza maksymalną wartość współczynnika przechwytywania wody i obszar przechwytujący krople. Przeprowadzono również obliczenia wpływu wybranych parametrów aerodynamicznych na ilość przechwytywanej wody przez profil.

Słowa kluczowe: przepływy dwufazowe, numeryczna mechanika płynów, osadzanie się wody.